Electronic Supplementary Material (ESI) for Materials Chemistry Frontiers.

Soft Nanohand Grabs a Growing Nanoparticle

Ken Cham-Fai Leung,[1,4] Xiao-Bo Li,[2,3] Xuan Li,[4] Siu-Fung Lee,[1,5] Jimmy C. Yu,[5] Paula M. Mendes,[6] Klaus E. Hermann,[2,7] Michel A. Van Hove*[2]*

[1] Department of Chemistry, The Hong Kong Baptist University, Kowloon Tong, Kowloon, Hong Kong

[2] Institute of Theoretical and Computational Studies, The Hong Kong Baptist University, Kowloon Tong, Kowloon, Hong Kong

[3] Hunan Key Laboratory of Super-Microstructure and Ultrafast Process, School of Physics and Electronics, Central South University, Changsha, China

[4] Faculty of Dentistry, The University of Hong Kong, Pokfulam, Hong Kong

[5] Department of Chemistry, The Chinese University of Hong Kong, Shatin, NT, Hong Kong

[6] School of Chemical Engineering, The University of Birmingham, Birmingham, United Kingdom

[7] Department of Inorganic Chemistry, Fritz-Haber-Institut der Max-Planck-Gesellschaft, Berlin, Germany

Electronic Supplementary Information (ESI)

Table of Contents

1. ESI Experimental Methods and Results

Third generation (G3) dendrons with three layers of branching points were synthesized from their smaller counterparts from second generation (G2) and first generation (G1) dendrons by a dendrimer convergent synthesis approach. All intermediately synthesized compounds were purified before performing the next reaction step. All reactions were performed under nitrogen atmosphere unless stated otherwise. Dichloromethane was pre-dried over CaH_2 and distilled under nitrogen. Dimethylformamide was pre-dried over magnesium sulfate and distilled under reduced pressure. Chromatography purifications were performed on silica gel (SiO_2) with the indicated eluents. All solvents were filtered through 0.2 μm membrane. All compounds were purchased from Sigma-Aldrich. ^{1}H and ^{13}C NMR spectra for structural characterization were recorded with Bruker Avance 400 (^{1}H: 400 MHz; ^{13}C: 101 MHz) spectrometer at 297 K. All NMR samples were dissolved in $CDCl_3$ unless otherwise stated. Spectra were calibrated internally using the solvent residual peak (e.g., for residual $CHCl_3$ in $CDCl_3$, ^{1}H: $\delta = 7.26$; ^{13}C: $\delta = 77.16$ ppm). Electrospray ionization (ESI) mass spectra were measured on a Bruker SolariX 9.4T mass spectrometer using CH_3OH/CH_2Cl_2 (1:1) as solvent. The reported mass-to-charge (*m/z*) values were corresponded to the most abundant monoisotopic masses. Matrix Assistant Laser Desorption Ionization iV Time of Flight Mass Spectrometer (MALDI-TOF-MS) was measured on a Bruker Autoflex MALDI-TOF MS. UV/V is absorption spectra were obtained using a Cary 5G UV-Vis-NIR spectrophotometer. Atomic force microscopy (AFM) was performed with scanning probe microscope (SPM) Veeco MultiMode IVa. Transmission electron microscope (TEM) and energy dispersive X-ray (EDX) were performed on a FEI TecnaiF20 field emission. Size measurement of gold nanoparticles (AuNPs) was calculated by PEBBLES. The dendritically wrapped AuNPs were also analyzed by BECKMAN COULTER Delsa^{TM}Nano HC particle size analyzer. These dendritically wrapped AuNPs were dissolved in DMF and further diluted with NaCl/EtOH solution (20 w%). Mobility and zeta potential analyses of the dendritically wrapped Au NPs (10 μg/mL) were performed for three times.

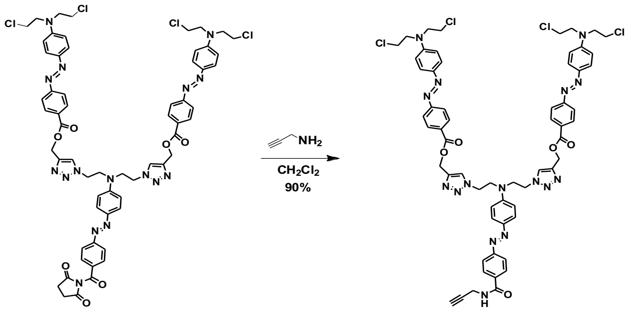

G2-2(NHS) **G2-3(acetylene)**

Figure S1. Synthesis of G2-3(acetylene) dendron.

G2-3(acetylene) dendron

G2-2(NHS) dendron (1.5 g, 1.1 mmol),[1,2] propargylamine (0.8 g, 14.5 mmol) were dissolved in anhydrous CH_2Cl_2 (20 mL). The reaction was carried out overnight. The precipitate was removed by filtration. The filtrate was washed with deionized water and the organic layer was collected and dried by anhydrous $MgSO_4$. The mixture was filtrated and then concentrated in vacuo. Then, it was purified by column chromatography with $CHCl_3$, then gradient to ethyl acetate as the eluents to afford the product as a liquid (1.2 g, 90%). ^{1}H NMR: 2.32 (t, *J* = 2.4 Hz, 1H, CCH), 3.69–3.76 (m, 12H, NCH_2CH_2), 3.86 (t, *J* = 6.8 Hz, 8H, $ClCH_2$), 4.25–4.28 (m, 2H, $CONCH_2$), 4.45 (t, *J* = 5.6 Hz, 4H, NCH_2) 5.41 (s, 4H, $COOCH_2NCH_2$), 6.64 (d, *J* = 9.2 Hz, 2H, ArH), 6.77 (d, *J* = 9.2 Hz, 4H, ArH), 7.55 (s, 2H, CH=C), 7.81–7.89 (m, 14H, ArH), 8.07 (d, *J* = 8.8 Hz, 4H, ArH). ^{13}C NMR: 28.6, 30.0, 31.6, 36.6, 40.4, 111.8, 112.3, 122.4, 122.8, 125.3, 125.9, 126.0, 128.1, 130.1, 130.8, 143.5, 144.8, 149.3, 156.0, 162.7, 166.1. HRMS (ESI): $C_{60}H_{58}Cl_4N_{16}O_5Na$ $[M+Na]^+$ calcd: 1247.3408, found: 1247.3385.

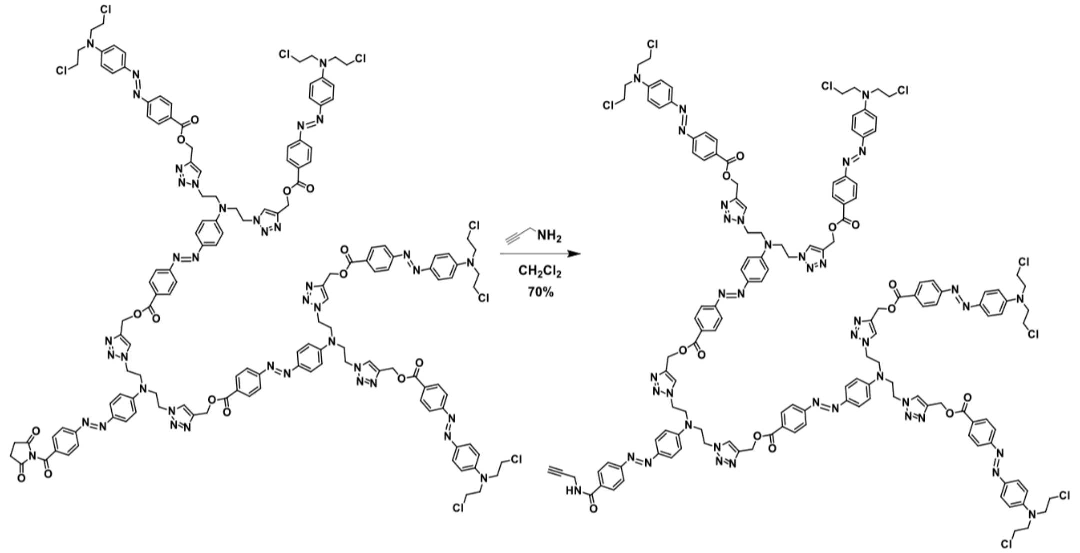

G3-2(NHS)　G3-3(acetylene)

Figure S2. Synthesis of G3-3(acetylene) dendron.

G3-3(acetylene) dendron

G3-2(NHS) dendron (1.5 g, 0.5 mmol),[1,2] propargylamine (0.8 g, 14.5 mmol) were dissolved in anhydrous CH_2Cl_2 (20 mL). The reaction was carried out for 2 d. The precipitate was removed by filtration. The filtrate was washed with deionized water and the organic layer was collected and dried by anhydrous $MgSO_4$. The mixture was filtrated and then concentrated in vacuo. Then, it was purified by column chromatography with $CHCl_3$, then gradient to ethyl acetate as the eluents to afford the product as a liquid (1.0 g, 70%). ^{1}H NMR: 2.29 (t, *J* = 2.8 Hz, 1H, CCH), 3.44–3.76 (m, 28H, NCH_2CH_2), 3.83–3.87 (m, 14H, $ClCH_2$), 4.03 (m, 2H, $ClCH_2$) 4.26–4.27 (m, 2H, $CONCH_2$), 4.46–4.66 (m, 12H, NCH_2) 5.41 (s, 12H, $COOCH_2$), 6.49–6.81 (m, 14H, ArH), 7.48–7.59 (m, 6H, CH=C), 7.68–7.89 (m, 30H, ArH), 7.99–8.09 (m, 12H, ArH). ^{13}C NMR (d_6-DMSO): 24.5, 25.4, 28.6, 30.7, 33.4, 41.0, 46.7, 47.6, 49.8, 52.0, 58.0, 111.7, 112.0, 122.1, 125.5, 125.9, 128.5, 129.6, 130.5, 142.0, 143.5, 150.2, 155.2, 156.7, 165.0. HRMS (ESI): $C_{140}H_{136}Cl_8N_{40}O_{13}$ $[M+2H]^{2+}$ calcd: 1434.9341, found: 1434.9340.

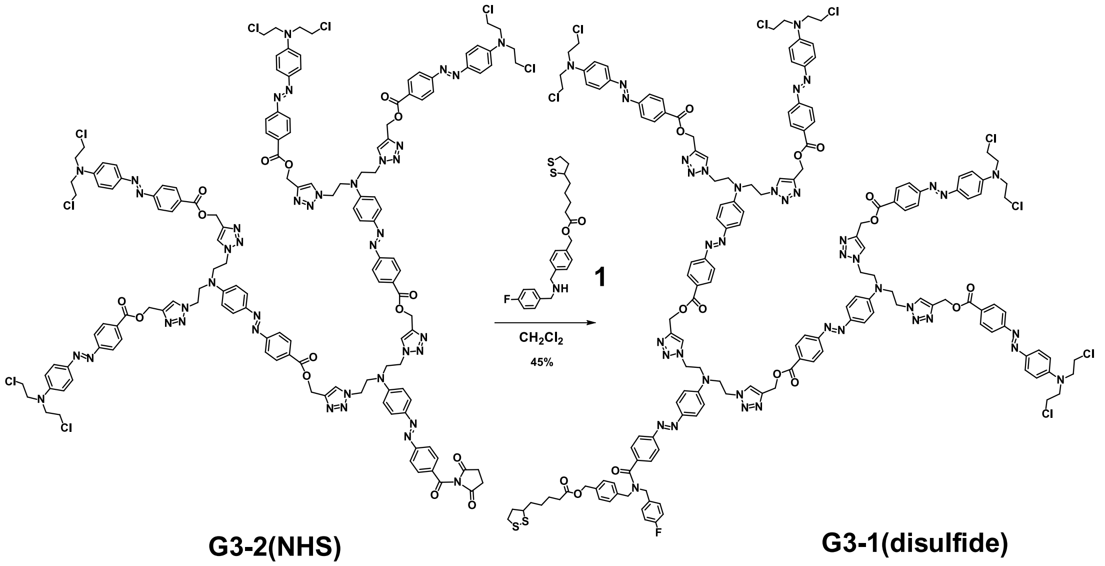

G3-2(NHS) **G3-1(disulfide)**

Figure S3. Synthesis of G3-1(disulfide) dendron.

G3-1(disulfide) dendron

G3-2(NHS) dendron (1.8 g, 0.6 mmol) and amine thread **1** (0.8 g, 1.85 mmol) were dissolved in anhydrous CH_2Cl_2 (20 mL).[1,2] The reaction was carried out for 2 days to achieve the highest yield. The precipitate was removed by filtration. The filtrate was washed with deionized water and the organic layer was collected and dried by anhydrous $MgSO_4$. The mixture was filtrated and then concentrated in vacuo. Then, it was purified by column chromatography with $CHCl_3$, then gradient to ethyl acetate as the eluents to afford the product as a liquid (0.88 g, 45%). ^{1}H NMR: 1.37–1.62 (m, 10H, CH_2CH_2), 2.04 (s, 2H, CH_2COO), 2.34–2.40 (m, 1H, CH_2CHS), 3.67–3.71 (m, 28H, NCH_2), 3.82–3.84 (m, 16H, $ClCH_2CH_2$), 4.42 (m, 14H, $ArCH_2N$), 4.46 (s, 2H, $ArCH_2N$), 5.11 (s, 1H, $ArCH_2$), 5.41 (s, 13H, $COOCH_2$, $ArCH_2$), 6.62–6.66 (m, 6H, ArH), 6.74 (d, J = 9.2 Hz, 8H, ArH), 6.99–7.05 (m, 2H, ArH), 7.33–7.35 (m, 2H, ArH), 7.51–7.59 (m, 8H, CH=C, ArH), 7.78–7.87 (m, 30H, ArH), 8.02–8.08 (m, 14H, ArH). ^{13}C NMR (d_6-DMSO): 40.4, 41.0, 49.8, 52.0, 58.0, 111.7, 112.0, 122.0, 125.5, 125.7, 129.6, 130.4, 142.0, 143.5, 150.1, 155.1, 165.0. HRMS (MALDI-TOF): $C_{160}H_{157}Cl_8FN_{40}O_{15}S_2Na$ $[M+Na]^+$ calcd: 3263.9584, found: 3265.9464.

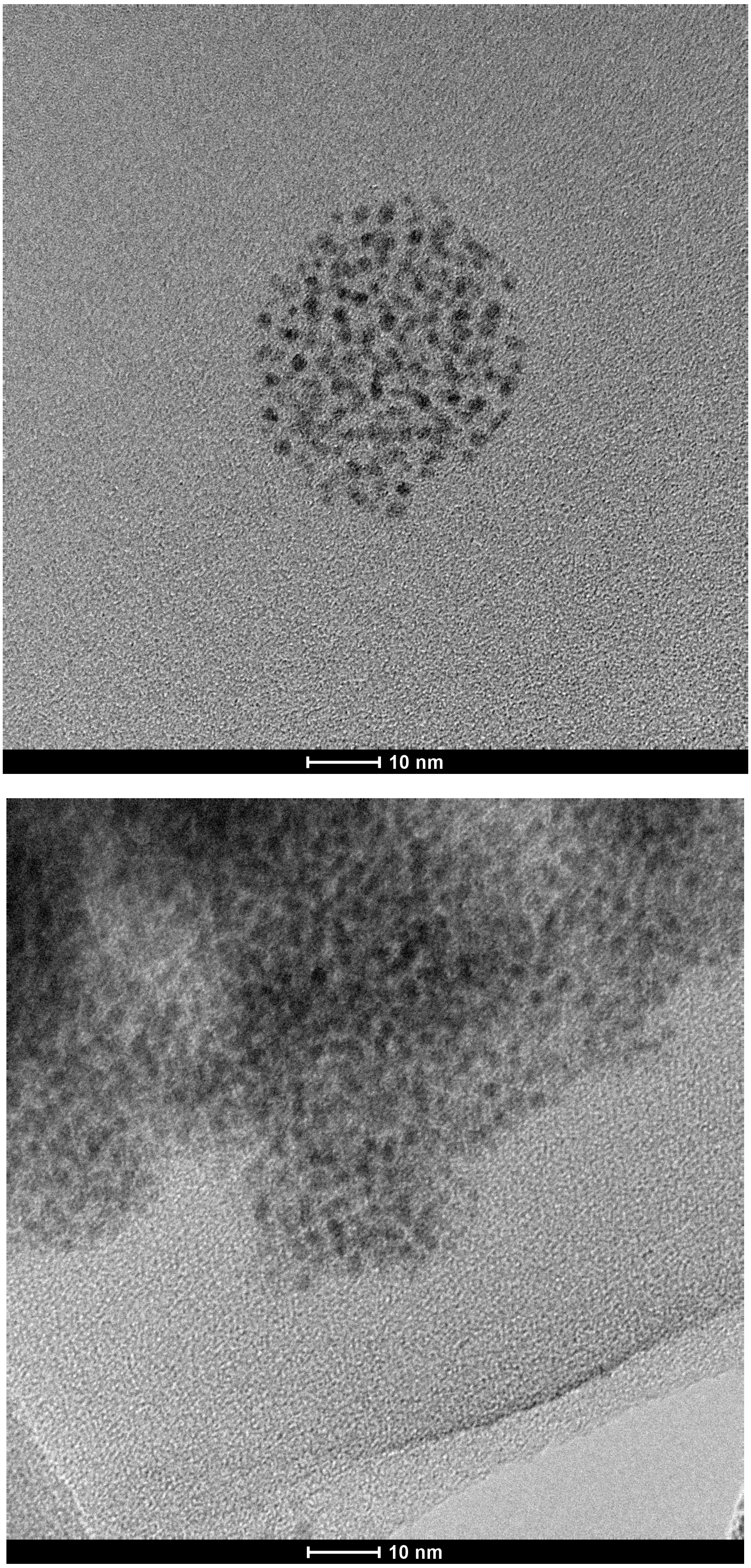

Figure S4. TEM images of G3-1(disulfide)@AuNP. Each dark spot of about 1.4 nm is a gold NP.

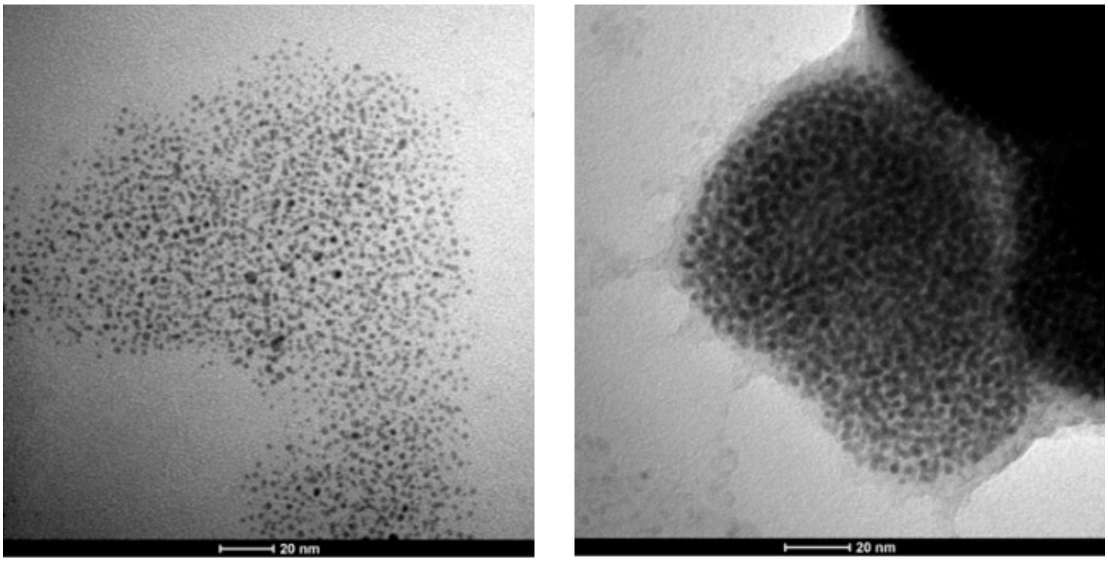

Figure S5. TEM images of G3-2(NHS)@AuNP (left) and G3-3(acetylene)@AuNP (right). Each dark spot of about 2.2-2.3 nm is a gold NP.

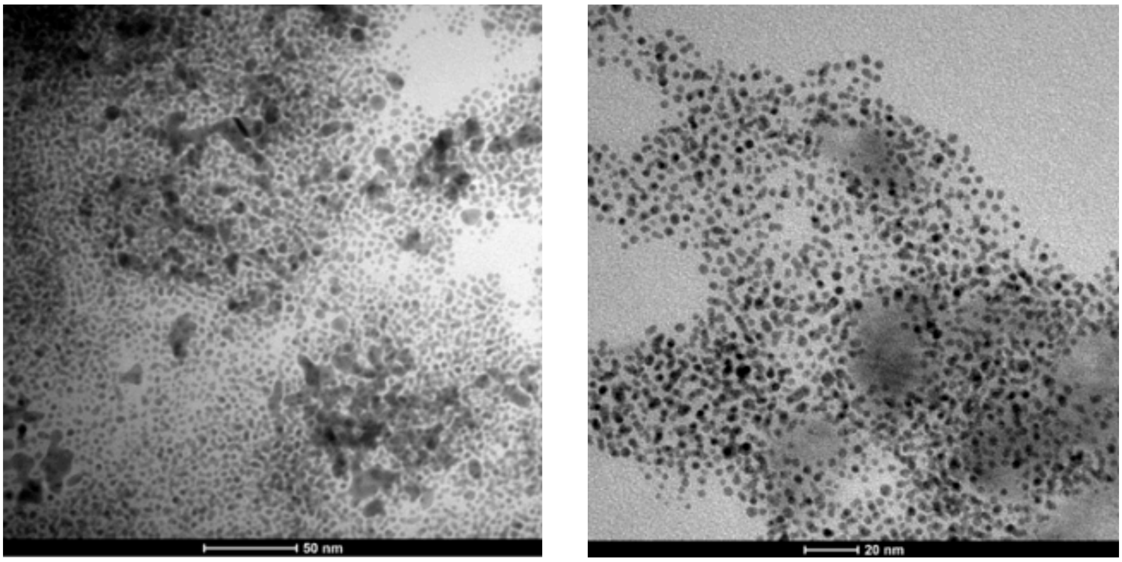

Figure S6. TEM images of G2-2(NHS)@AuNP (left) and G2-3(acetylene)@AuNP (right).

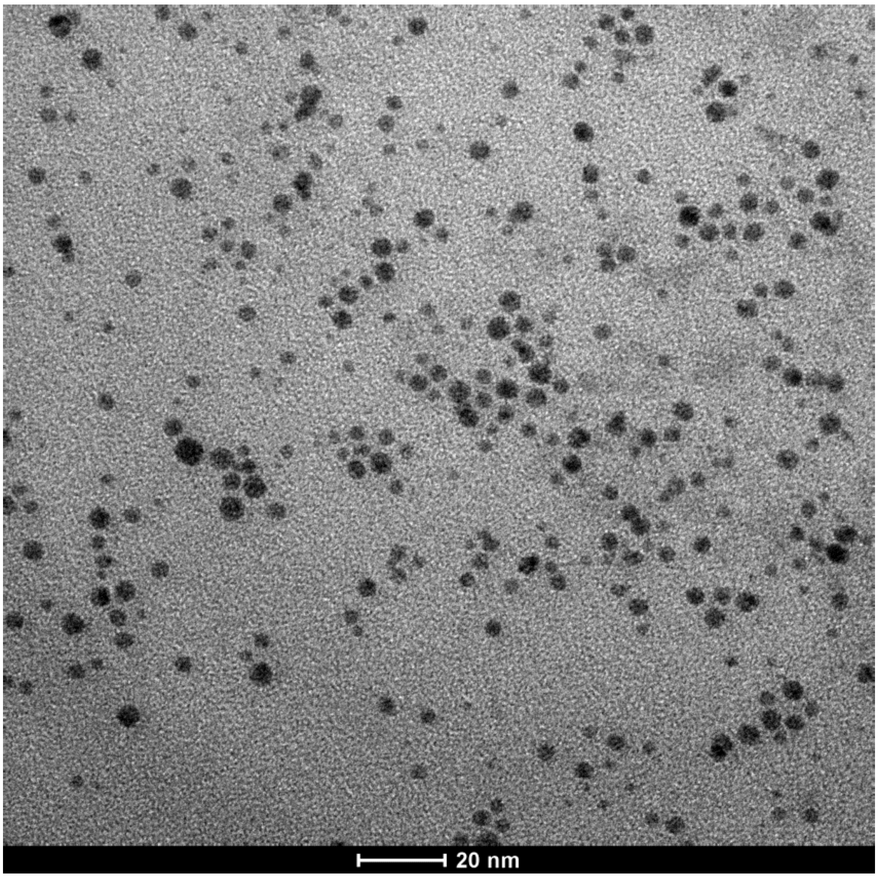

Figure S7. TEM image of Au NP synthesis without the dendron (control).

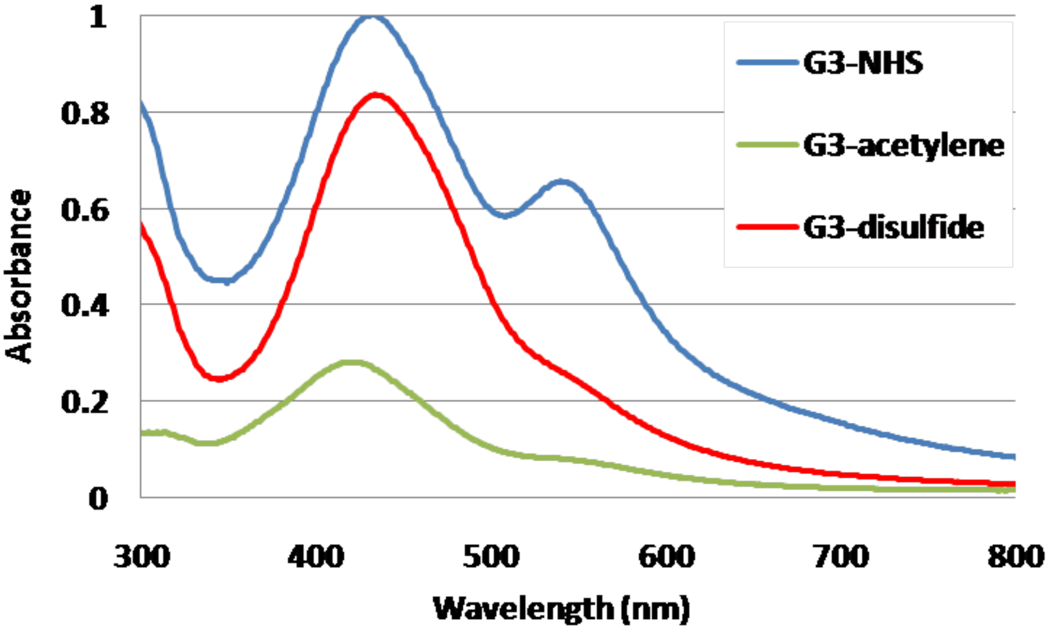

Figure S8. UV-visible absorption spectra of the three different G3(NHS, acetylene, and disulfide)-dendritically wrapped Au NPs.

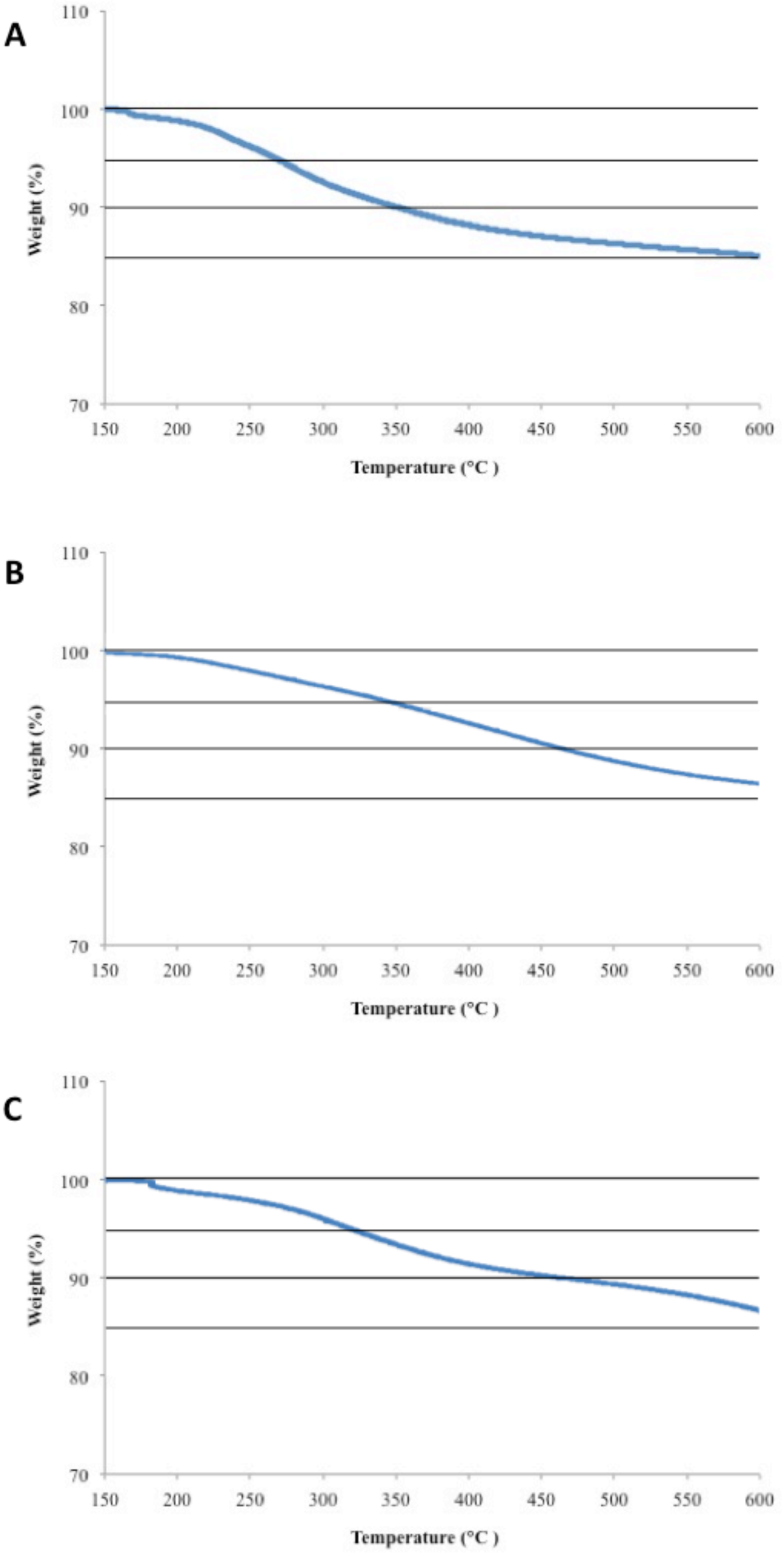

Figure S9. Thermogravimetric analysis (TGA) spectra (150–600 ºC) of (A) G3-1(disulfide)@AuNP; (B) G3-2(NHS)@AuNP; and (C) G3-3(acetylene)@AuNP.

Table S1. Estimation of the number of Au atom according to the Au NP size by $N = 30.9d^3$ where N is the number of Au atom and d is the average diameter (nm) of Au NPs.[3–5]

Estimated number of Au atom	Au NP size, diameter (nm)
85	1.4
329	2.2
376	2.3

Table S2. Molecular weights of separate components in the dendritically wrapped Au NP structures.

Component	Molecular weight (gmol^{-1})
Au_{85}	16,742.16
G3(disulfide) dendron ($C_{160}H_{157}Cl_8FN_{40}O_{15}S_2$)	3,247.00
Au_{329}	64,802.00
G3(NHS) dendron ($C_{141}H_{134}Cl_8N_{40}O_{16}$)	2,928.49
Au_{376}	74,059.43
G3(acetylene) dendron ($C_{140}H_{134}Cl_8N_{40}O_{13}$)	2,868.48

Table S3. Estimated weight percentages of dendron (organic) and gold (inorganic) with the 1:1 dendritically wrapped Au NP having a single dendron wrapping a single Au NP (calculated using the molecular weights of separate components in Table S2).

1:1 Organic-inorganic hybrid structure	Weight% dendron	Weight% gold
G3(disulfide)-Au_{85}NP	16.2	83.8
G3(NHS)-Au_{329}NP	4.3	95.7
G3(acetylene)-Au_{376}NP	3.7	96.3

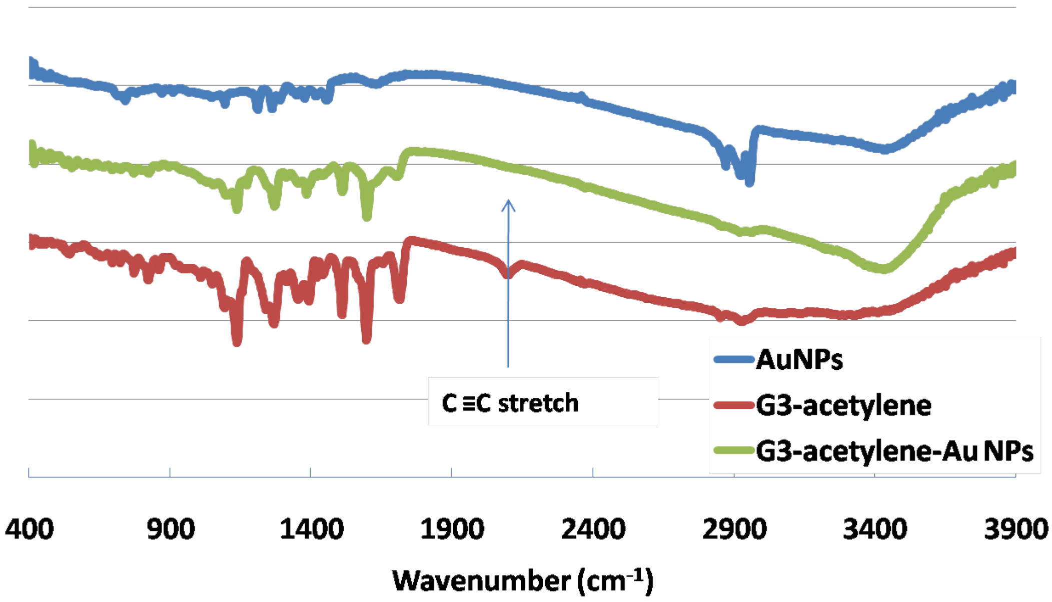

Figure S10. Infrared spectra of the bare AuNPs, G3-3(acetylene) dendron, and G3-3(acetylene)@AuNP.

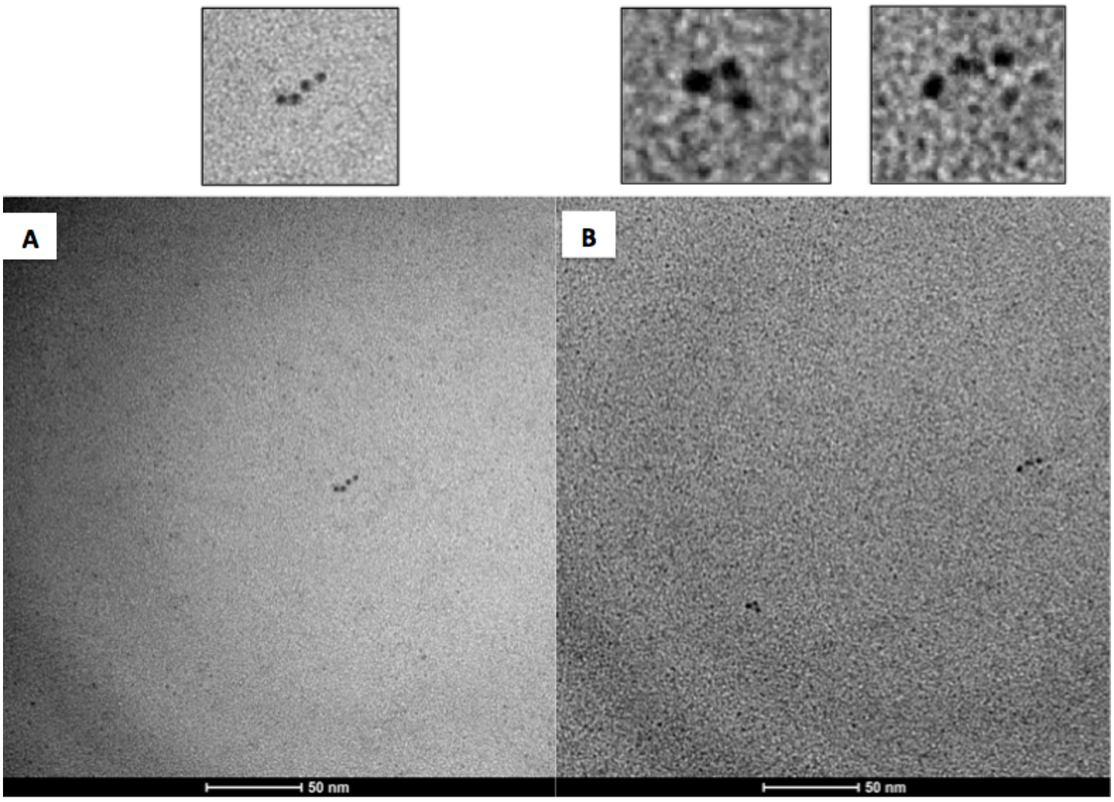

Figure S11. TEM and magnified images of G3-3(acetylene)@AuNP oligomers after homo-coupling reaction with a $Pd(PPh_3)_2Cl_2$ catalyst and triethylamine.

NMR Spectra:

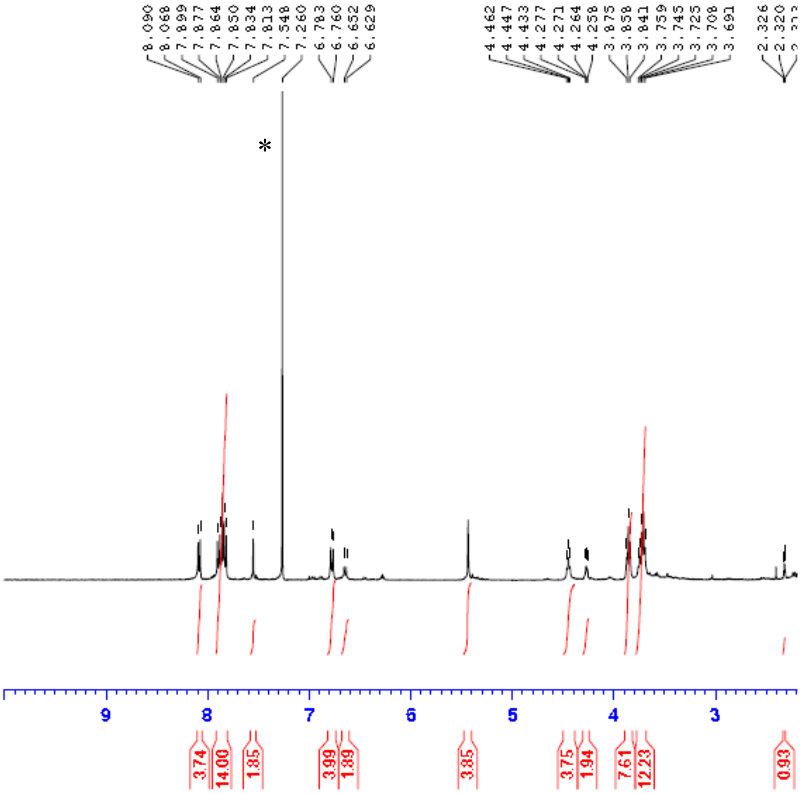

Figure S12. ^{1}H NMR spectrum of G2-3(acetylene) dendron (*solvent residue).

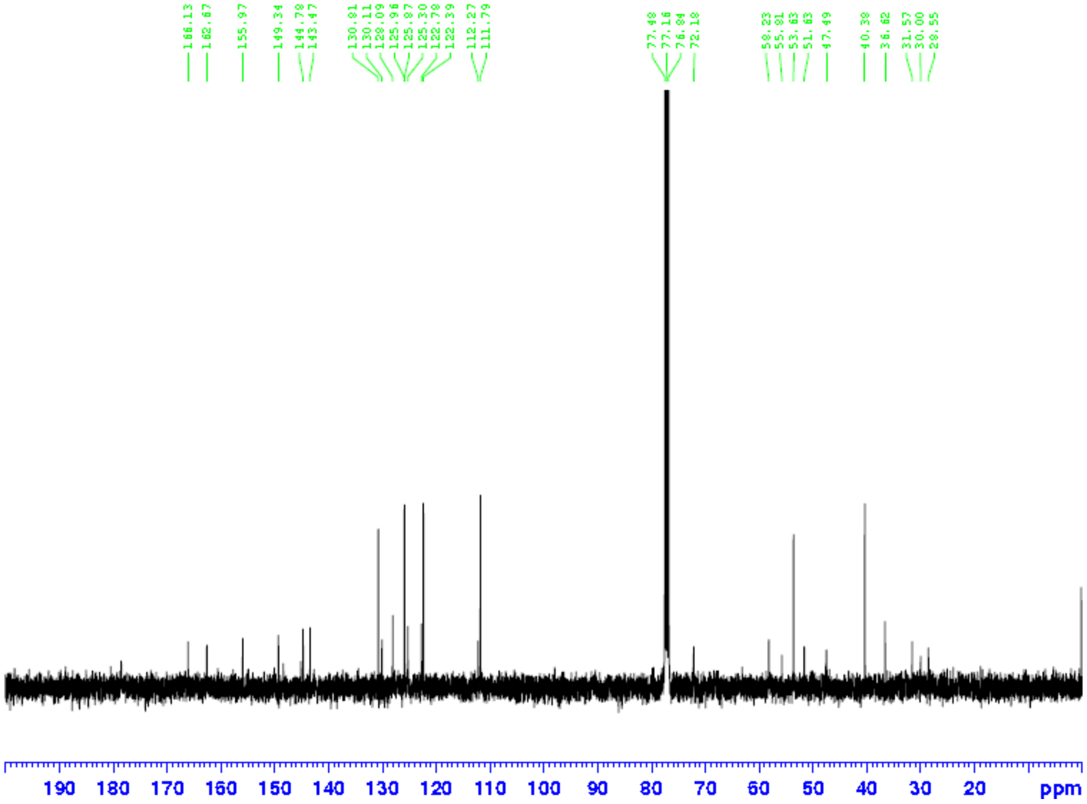

Figure S13. ^{13}C NMR spectrum of G2-3(acetylene) dendron.

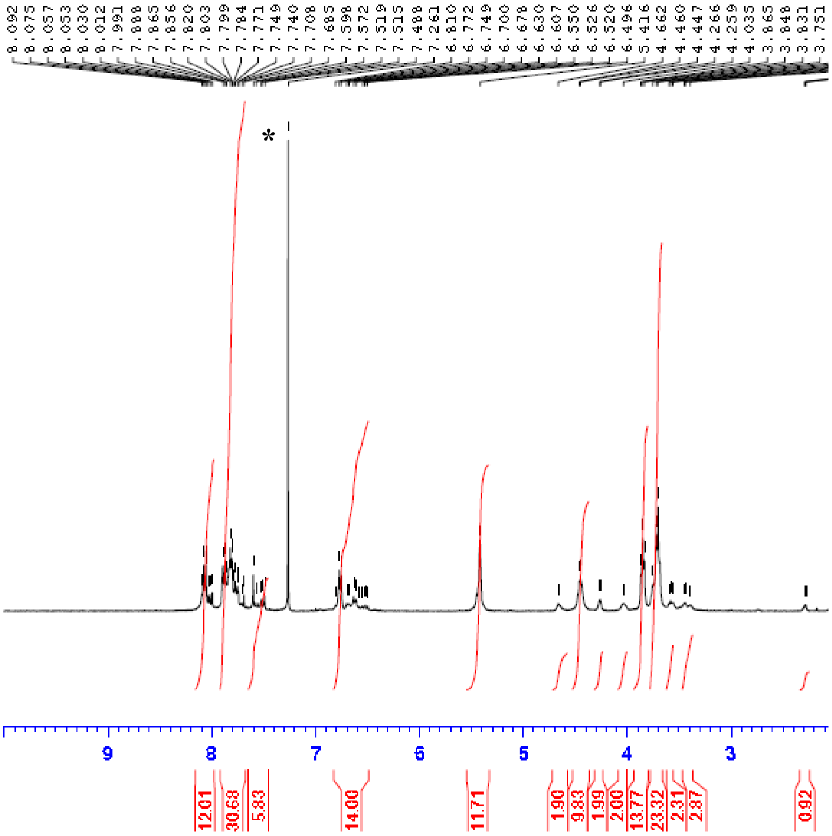

Figure S14. ^{1}H NMR spectrum of G3-3(acetylene) dendron (*solvent residue).

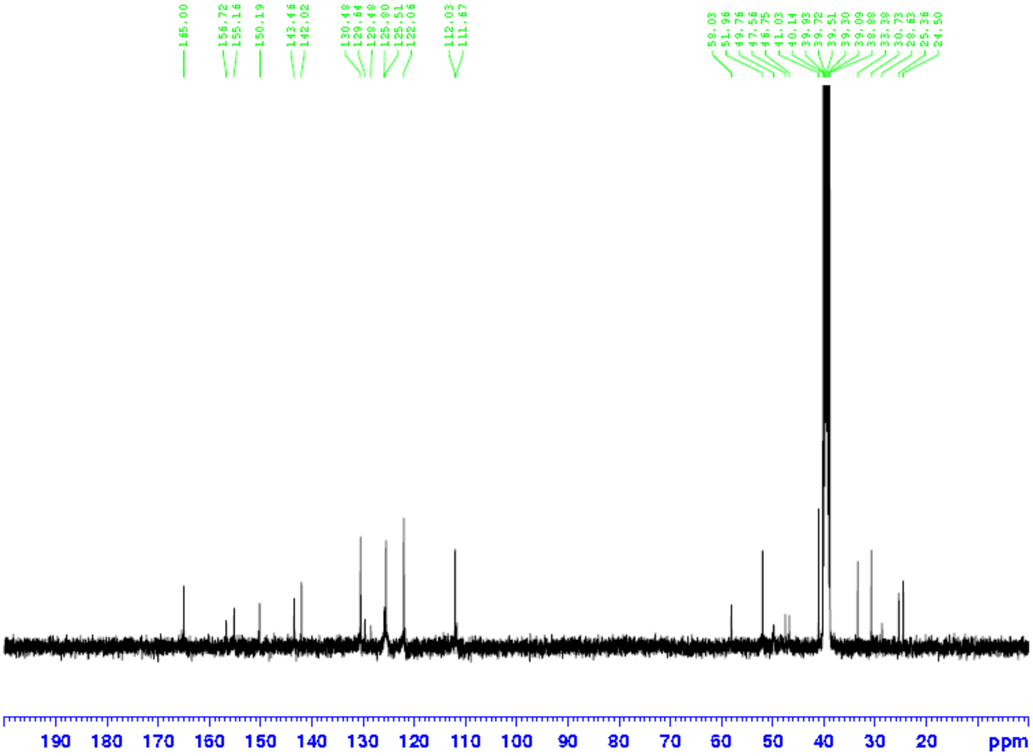

Figure S15. ^{13}C NMR spectrum of G3-3(acetylene) dendron (*d*-DMSO).

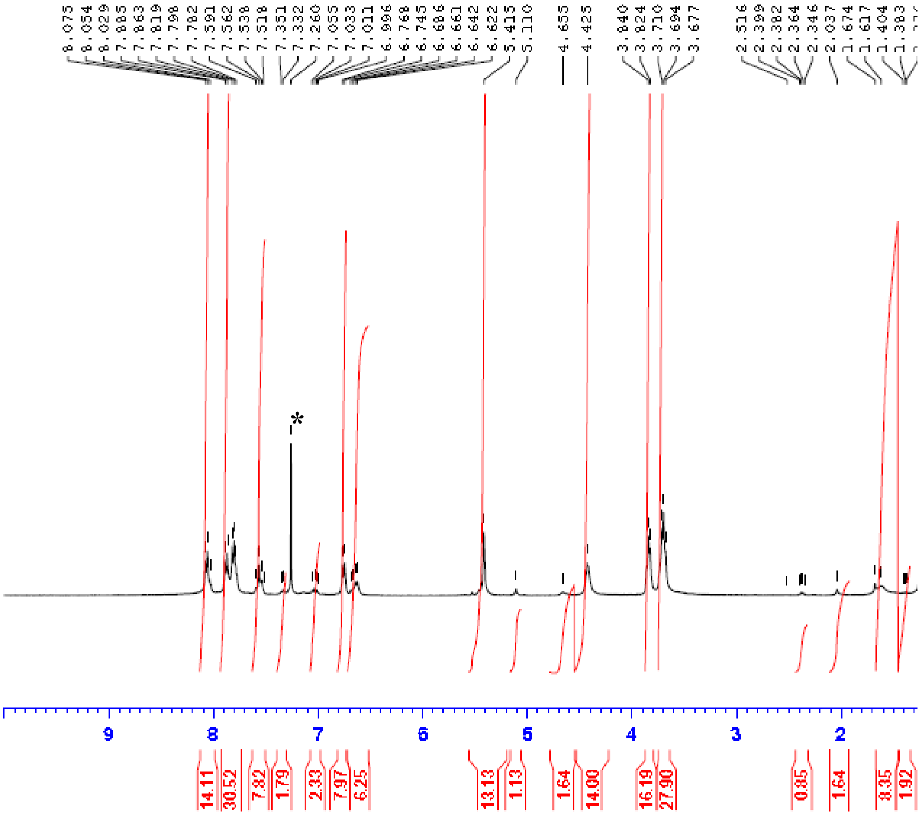

Figure S16. ^{1}H NMR spectrum of G3-1(disulfide) dendron (*solvent residue).

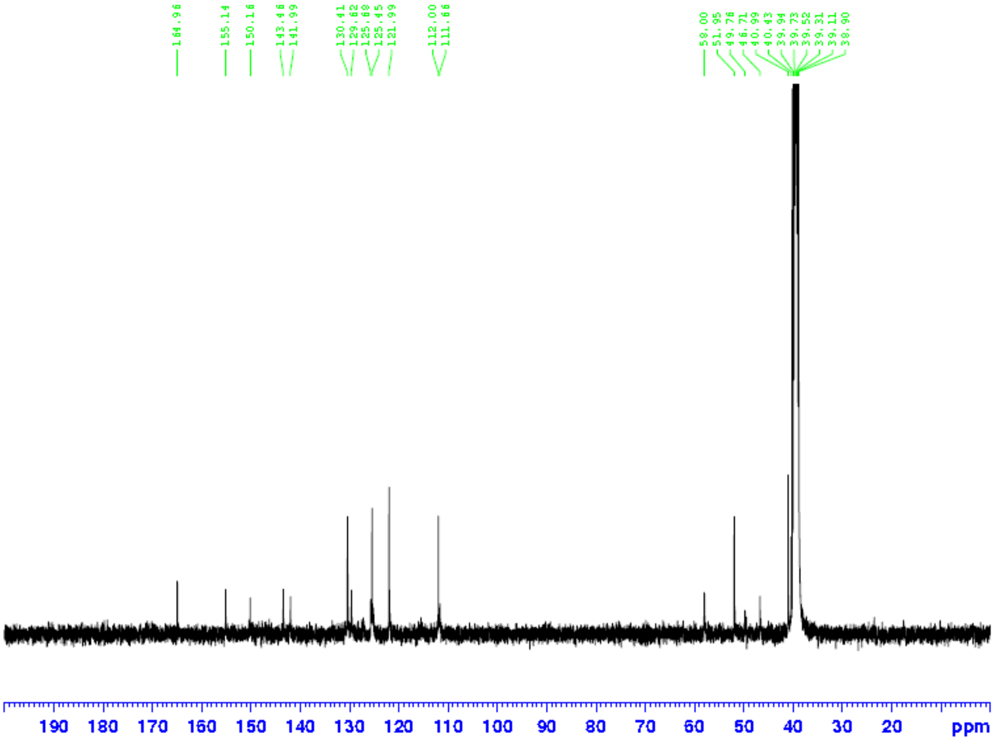

Figure S17. ^{13}C NMR spectrum of G3-1(disulfide) dendron (*d*-DMSO).

2. ESI Theoretical Methods, Energetics

In terms of energetics, one cannot directly compare total energies between systems that have different numbers and/or kinds of atoms: this is the case here, since the three anchor groups are very different in this respect. However, one can compare binding energies, which are derived as differences of total energies for clusters having the same number of atoms and identical atom types.

We describe here how we calculate binding energies of the dendrons to the Au NPs, including the distinction between "bonding energy" and "deformation energy". For this purpose, we define binding and deformation energies, starting from the total energies of gold NPs (denoted Au_n, whether for Au_{78}, Au_6 or Au_8) and dendrons (denoted G3; this includes the cases of truncated and H-terminated anchor groups denoted G3-A above), as follows:

- $E_{tot}(Au_n) < 0$ is the total energy of an isolated gold NP in its optimized geometry (a local energy minimum starting from its geometry in an optimized G3@Au_n cluster, not necessarily reflecting a global energy minimum).
- E_{tot} (G3) < 0 is the total energy of an isolated dendron in its optimized geometry (a local energy minimum starting from its geometry in an optimized G3@Au_n cluster).
- $E_{tot}(G3@Au_n) < 0$ is the total energy of the combined gold NP and dendron cluster in its optimized geometry (a local energy minimum).
- $E_{tot}^{frozen}(Au_n) > E_{tot}(Au_n)$ is the total energy of a geometrically "frozen" gold NP with its geometry taken from that in the optimized G3@Au_n cluster. This structure does <u>not</u> correspond to a local energy minimum of the NP, but serves as starting point to reach the abovementioned locally optimized structure with total energy $E_{tot}(Au_n)$.
- $E_{tot}^{frozen}(G3) > E_{tot}(G3)$ is the total energy of a geometrically "frozen" dendron with its geometry taken from that in the optimized G3@Au_n cluster. This structure does <u>not</u> correspond to a local energy minimum of the dendron, but serves as starting point to reach the abovementioned locally optimized structure with total energy $E_{tot}(G3)$.

Clearly, all total energies defined above are evaluated self-consistently, i.e. equilibrated electronically where the energies $E_{tot}(Au_n)$, $E_{tot}(G3)$ and $E_{tot}(G3@Au_n)$ include also geometric optimization in contrast to $E_{tot}^{frozen}(Au_n)$ and $E_{tot}^{frozen}(G3)$. From the total energies defined above, we evaluate the various binding and deformation energies as follows:

- The fully optimized binding energy E_b between a gold NP and a dendron is defined by

$$E_b = E_{tot}(G3@Au_n) - E_{tot}(Au_n) - E_{tot}(G3) < 0$$

It combines both bonding effects and geometric deformations (conformational changes) of the two components of G3@Au_n when they bind with each other.

- The geometrically frozen binding energy E_b^{frozen} between a gold NP and a dendron is defined by

$$E_b^{frozen} = E_{tot}(G3@Au_n) - E_{tot}^{frozen}(Au_n) - E_{tot}^{frozen}(G3) < E_b$$

This binding energy, also called "bonding energy" above, ignores geometric deformation of the separated components as a result of interactive coupling with $E_b^{frozen} < E_b < 0$. It includes only bond breaking, charge separation (if there is polarization between gold NP and dendron), and other similar electronic effects.

- The deformation energy $E_{deform}(Au_n)$ of a gold NP is defined by

$$E_{deform}(Au_n) = E_{tot}^{frozen}(Au_n) - E_{tot}(Au_n) > 0$$

It compares the total energy of a geometrically "frozen" gold NP with its geometry taken from that in the optimized G3@Au_n cluster with the total energy of the same gold NP which is geometrically re-optimized, see above. Therefore, $E_{deform}(Au_n)$ reflects structural deformation (including any resulting internal electronic relaxation) of the Au NP due to separation from the dendron.

- The deformation energy $E_{deform}(G3)$ of a dendron is defined by

$$E_{deform}(G3) = E_{tot}^{frozen}(G3) - E_{tot}(G3) > 0$$

It is conceptually equivalent to $E_{deform}(Au_n)$ but refers to structural deformation of the separated dendron rather than the separated Au NP.

The fully optimized binding energy E_b is related to the geometrically frozen binding energy ("bonding energy") E_b^{frozen} and the geometric deformation energies

$E_{deform}(Au_n)$ and $E_{deform}(G3)$ as follows:

$$E_b = E_b^{frozen} + E_{deform}(Au_n) + E_{deform}(G3)$$

This relation decomposes the total binding energy between gold NP and dendron into an “electronic bonding” (geometrically frozen) energy and geometric deformation (geometrically optimized) energies for the separated NP and dendron.

3. Compact Nanoparticle Structure, Polyhedral Fcc (*k, m*) Nanoparticles (NPs)

We consider highly symmetrical polyhedral atom clusters, denoted (*k, m*), of internal fcc lattice structure as simple models of the Au nanoparticles (NP). These are confined by six (100) facets of square shape, having $k\times k$ atoms each, and eight (111) facets of hexagonal shape, each of which has alternating *k* and *m* atom edges ($k\times m$ hexagons). Here (1, *m*) NPs are of octahedral shape while (*k, m*) NPs with $k > 1$ can be considered truncated octahedral, originating from a larger (1, m+2k-2) octahedral NP by cutting off (k-1)×(k-1) square pyramidal atom clusters at its 6 corners, see ESI Figure 18.

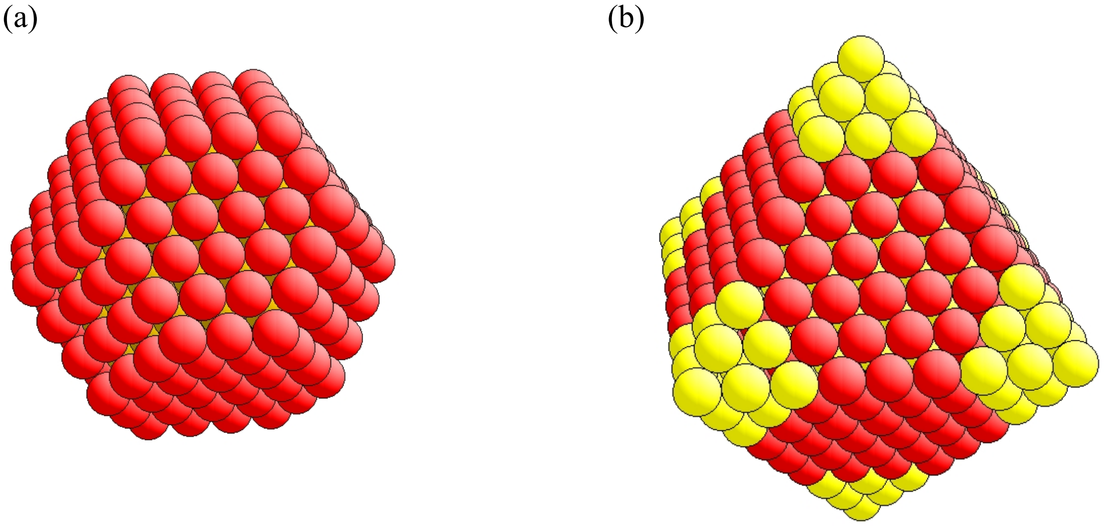

Figure S18. Geometric structure of polyhedral NPs of internal fcc lattice structure: (a) a truncated octahedral (4, 3) NP of 405 atoms, (b) an octahedral (1, 9) NP of 489 atoms; truncation by removing the six 3×3 square pyramidal atom clusters (yellow atom balls) at its corners, yields the (4,3) NP.

Simple lattice theory shows that the number of atoms in the (*k, m*) NP with $k, m \geq 1$ is given by

$$N_{tot}(k,m) = \frac{1}{3}(2k+m-3)(2k+m-2)\left[2(2k+m-3)+1\right] + (2k+m-2)^2 - (k-1)k(2k-1) \qquad (1)$$

while the number of atoms in its outer polyhedral shell confining the NP for $(k, m) \neq (1, 1)$ (describing an atom), is given by

$$N_{shell}(k,m) = 4(2k+m-3)^2 - 6(k-1)^2 + 2 \tag{2}$$

The diameter of the (k, m) NP, defined by the largest distance between atomic nuclei of the NP, identical with the diameter of the smallest sphere circumscribing the NP, is given by

$$D(k,m) = a\sqrt{(k+m-2)^2 + (k-1)^2} \tag{3}$$

where a is the lattice constant of the fcc lattice, $a = 0.407$ nm for gold, also used in the following.

The polyhedral surface of the (k, m) NP, defined by the summed area of confining (1 1 1) and (1 0 0) facets, is given by

$$A(k, m) = a^2\left[\sqrt{3}(m-1)(m+4k-5) + \left(3+\sqrt{3}\right)(k-1)^2\right] \tag{4}$$

while the spherical surface, defined by the smallest sphere enclosing the NP, is given by

$$A_s(k,m) = \pi D(k,m)^2 = \pi a^2\left((m+k-2)^2 + (k-1)^2\right) \tag{5}$$

ESI Table 4 lists results for selected (k, m) NPs which appear in the paper.

Table S4. Numerical results for N_{tot}, N_{shell}, D/a, D, A, and A_s of selected (k, m) NPs according to (1) - (5). The diameter D and areas A, A_s are calculated using the lattice constant for fcc gold, $a = 0.407$ nm.

(k, m)	N_{tot}	N_{shell}	D/a	D [nm]	A [nm]	A_s [nm]
(3, 2)	116	78	$\sqrt{13}$	1.467	5.718	6.799
(3, 3)	201	122	$\sqrt{20}$	1.820	8.874	10.459
(4, 2)	260	144	$\sqrt{25}$	2.035	10.785	13.074
(4,3)	405	204	$\sqrt{34}$	2.373	15.088	17.781

Growing a (k, m) NP by adding an outer polyhedral shell leads to a (k', m') NP where for

$k > 1$ $\quad (k, m) \rightarrow (k', m') = (k + 1, m)$, $\quad m > 0$ (6a)

$k = 1$ (octahedral NP) $\quad (1, m) \rightarrow (1, m') = (1, m + 2)$, $\quad m > 2$ (6b)

Peeling of a (k, m) NP by removing an outer polyhedral shell is inverse to shell addition. Relations (6a, b) show that a direct transition from (3, 2) to (4, 3) NPs cannot be achieved by adding or removing complete polyhedral shells only. However, the transition from a (3, 2) NP to a (4, 3) NP can be realized in two steps, first adding a partial shell to the (3, 2) NP to yield (3, 3), followed by a complete shell addition to yield the (4, 3) NP, see ESI Figure 19.

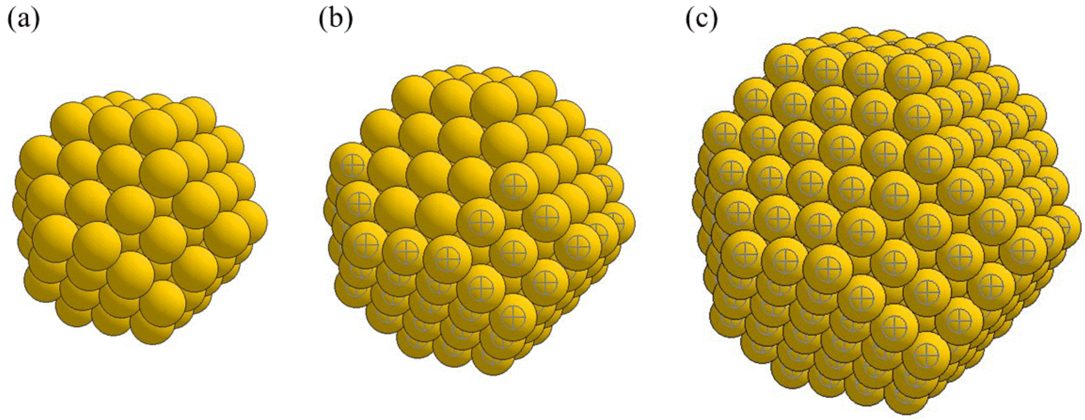

Figure S19. Geometric structure of polyhedral fcc Au NP (the same scale is used to draw the 3 NPs): (a) Au (3, 2) of 116 atoms, (b) Au (3, 3) of 201 atoms (surface atoms included by partial shell addition to Au (3, 2) are labeled), (c) Au (4, 3) of 405 atoms (surface atoms included by full shell addition to Au (3, 3) are labeled).

Alternatively, the transition from a (3, 2) NP to a (4, 3) NP can be realized in two steps by first adding a complete shell to the (3, 2) NP to yield (4, 2), followed by a partial shell addition to yield the (4, 3) NP, see ESI Figure 20.

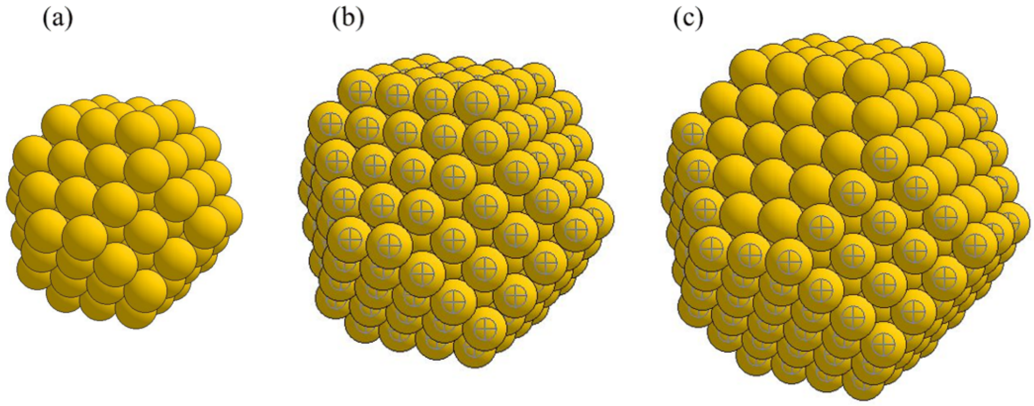

Figure S20. Geometric structure of polyhedral fcc Au NP (the same scale is used to draw the 3 NPs): (a) Au (3, 2) of 116 atoms, (b) Au (4, 2) of 260 atoms (surface atoms included by full shell addition to Au (3, 2) are labeled), (c) Au (4, 3) of 405 atoms (surface atoms included by partial shell addition to Au (4, 2) are labeled).

4. Movies of Large G3@Au_{78} Clusters

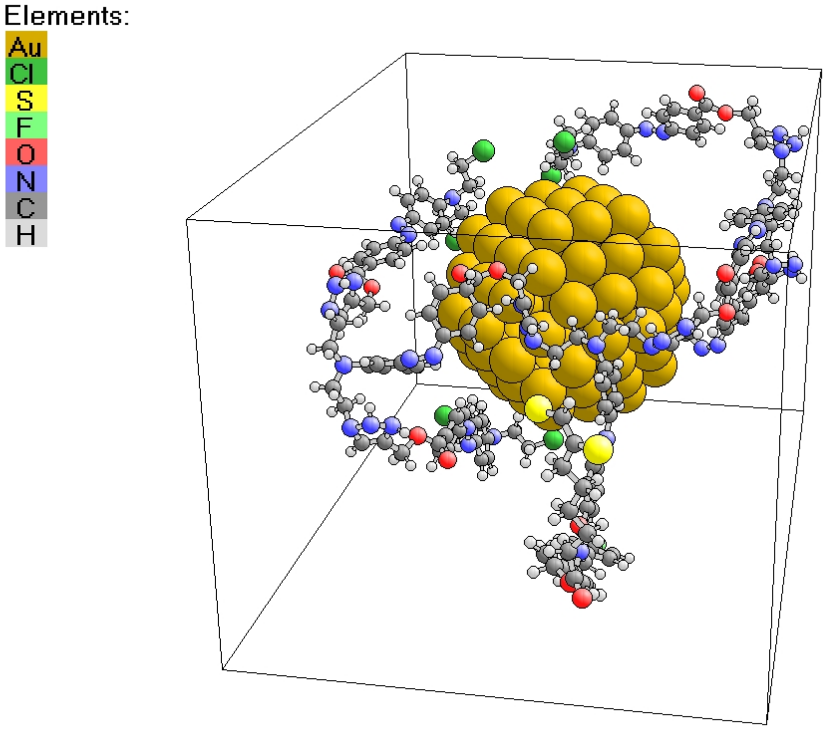

Figure S21. Starting frame of movie MovS1_Au78DeG31movie.mp4 showing perspective views of cluster G3-1@Au_{78}.

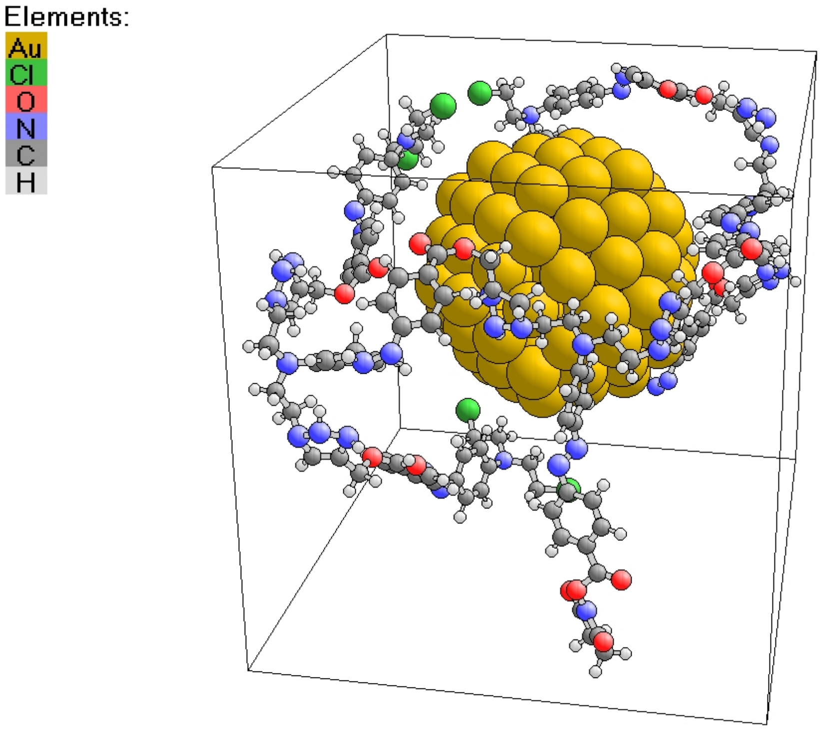

Figure S22. Starting frame of movie MovS2_Au78DeG32movie.mp4 showing perspective views of cluster G3-2@Au_{78}.

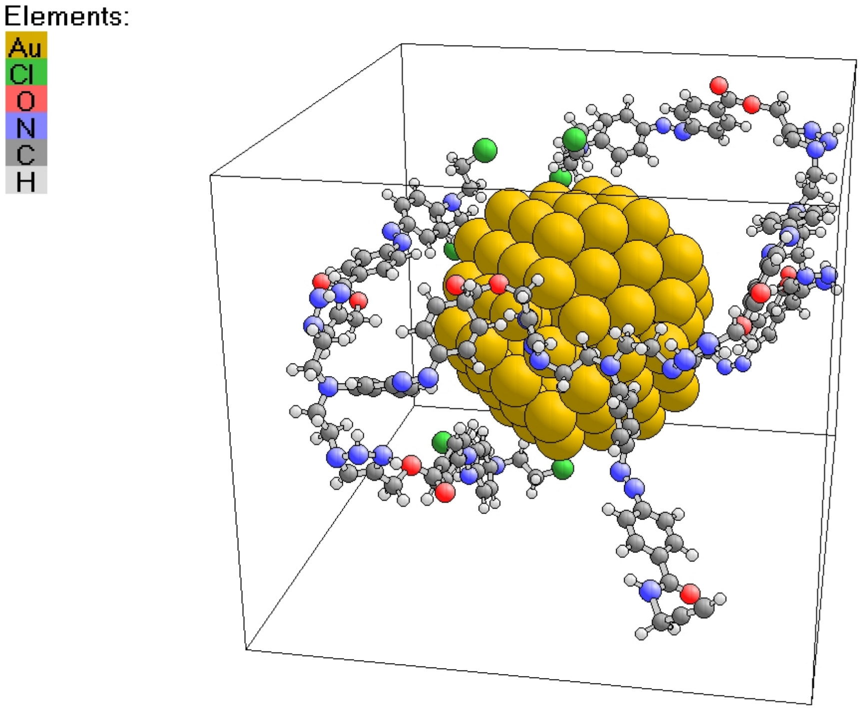

Figure S23. Starting frame of movie MovS3_Au78DeG33movie.mp4 showing perspective views of cluster G3-3@Au_{78}.

5. Structures and Energies of Small G3-A@Au$_n$ Clusters (n = 6, 8)

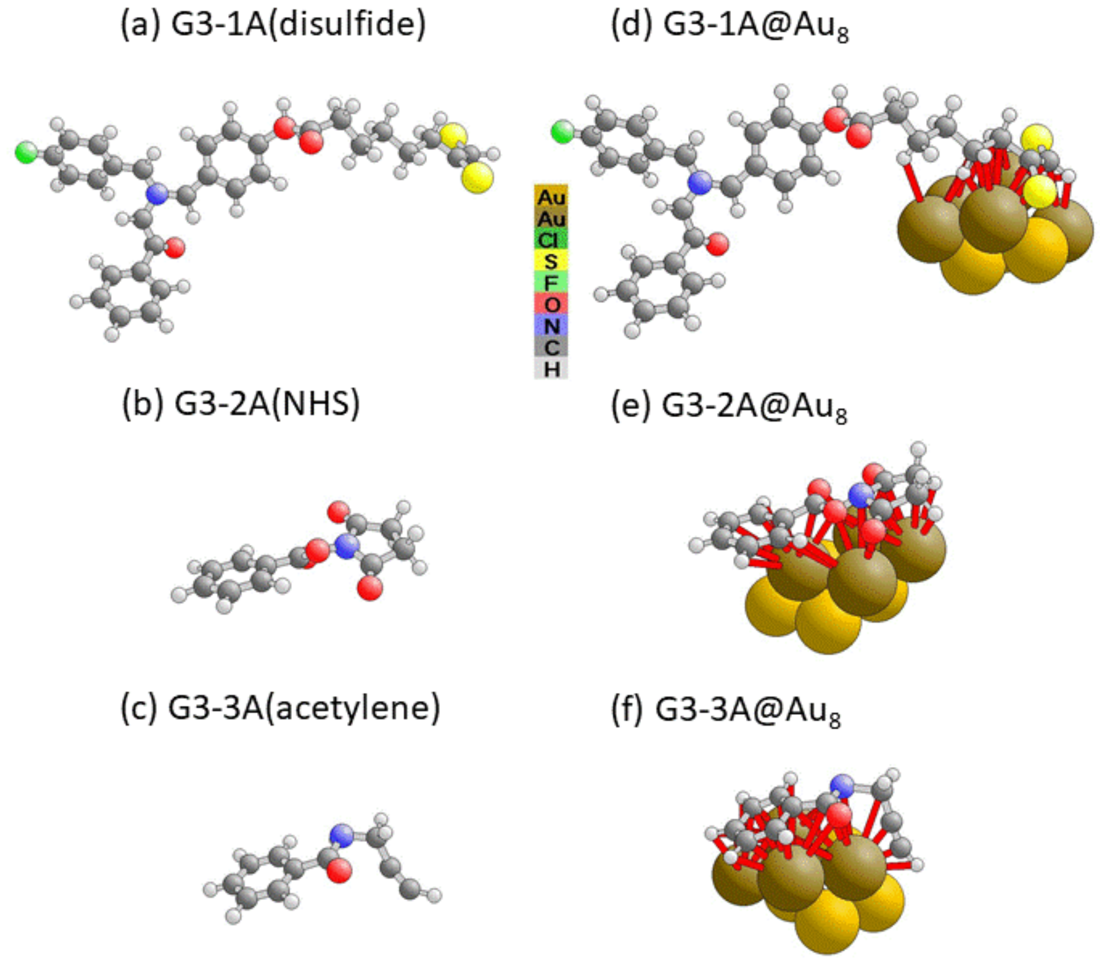

(a) G3-1A(disulfide)

(d) G3-1A@Au$_8$

(b) G3-2A(NHS)

(e) G3-2A@Au$_8$

(c) G3-3A(acetylene)

(f) G3-3A@Au$_8$

Figure S24. Perspective views of ball-and-stick models of three dendron anchor molecules G3-1A, G3-2A, and G3-3A (a-c), shown with their structures taken from the corresponding geometry-optimized Au-dendron clusters G3-1A@Au$_8$, G3-2A@Au$_8$, and G3-3A@Au$_8$ (d-f), see text. The red interatomic links refer to Au-dendron internuclear distances up to 0.4 nm, with dendron-linked gold atoms emphasized by darker color (brown).

Table S5. Minimum distances d_{min} of gold – dendron anchor bond links for three different G3-A@Au_6 and G3-A@Au_8 clusters, see text. Entries "-" denote that the corresponding link distances are above 0.4 nm; entries "na" mean that the corresponding links do not appear in the cluster.

Bond link	**G3-1A@Au_n** **n = 6 / 8**	**G3-2A@Au_n** **n = 6 / 8**	**G3-3A@Au_n** **n = 6 / 8**
Au–H	0.250 / 0.230	0.223 / 0.271	0.283 / 0.252
Au–C	0.225 / 0.278	0.272 / 0.227	0.216 / 0.225
Au–N	- / -	0.356 / 0.350	0.340 / 0.358
Au–O	- / -	0.237 / 0.281	0.309 / 0.300
Au–F	- / -	na / na	na / na
Au–S	0.233 / 0.232	na / na	na / na

Table S6. Number (frequency of occurrence) of Au–dendron anchor bond links below 0.4 nm for three different G3-A@Au_6 and G3-A@Au_8 clusters, see text. Entries "na" mean that the corresponding links do not appear in the cluster.

Bond link	**G3-1A@Au_n** **n = 6 / 8**	**G3-2A@Au_n** **n = 6 / 8**	**G3-3A@Au_n** **n = 6 / 8**
Au–H	7 / 10	6 / 6	9 / 12
Au–C	9 / 9	10 / 15	16 / 24
Au–N	0 / 0	3 / 3	3 / 2
Au–O	0 / 0	6 / 10	2 / 2
Au–F	0 / 0	na / na	na / na
Au–S	4 / 2	na / na	na / na

Table S7. Binding and deformation energies for three different G3-A@Au_6 and G3-A@Au_8 clusters, and their Au and dendron components G3-A, see text. For definitions of the energy contributions see Sec. **ESI Theoretical Methods, Energetics**.

Energy (eV)	**G3-1A@Au_n** **n = 6 / 8**	**G3-2A@Au_n** **n = 6 / 8**	**G3-3A@Au_n** **n = 6 / 8**
E_b	–2.39 / –2.83	–0.92 / –0.82	–0.91 / –0.64
E_b^{frozen}	–4.19 / –4.40	–5.17 / –1.68	–2.80 / –1.66
$E_{deform}(Au_n)$	0.48 / 0.90	0.36 / 0.58	0.50 / 0.39
E_{deform}(G3-A)	1.32 / 0.66	3.88 / 0.28	1.39 / 0.63

6. References

[1] S.-F. Lee, Q. Wang, D. K.-L. Chan, P.-L. Cheung, B. S. Ong, K.-W. Wong, J. C.Yu, K. C.-F. Leung, *New J. Chem.* **2014,** *38*, 3362.

[2] Q. Wang, S.-F. Lee, C. Y. Tang, K. C.-F. Leung, K.-W. Wong, *RSC Adv.* **2014**, *4*, 18193.

[3] D. Thompson, J. P. Hermes, A. J. Quinn, M. Mayor, *ACS Nano* **2012**, ***6***, 3007.

[4] F. Sander, U. Fluch, J. P. Hermes, M. Mayor, *Small* **2014**, *10*, 349.

[5] J. P. Hermes, F. Sander, U. Fluch, T. Peterle, D. Thompson, R. Urbani, T. Pfohl, M. Mayor, *J. Am. Chem. Soc.* **2012**, *134*, 14674.